

## UNEXPECTEDLY LARGE S ISOTOPE FRACTIONATION DURING NATURAL SULFIDE OXIDATION AT COLD TEMPERATURES

K.J. Rodzinyak<sup>1,3</sup>, B.A. Wing<sup>2</sup>, R.J. Léveillé<sup>3</sup>, <sup>1,2</sup>Earth and Planetary Sciences, McGill University, Montréal, Québec. (kristyn.rodzinyak@mail.mcgill.ca), <sup>3</sup>Canadian Space Agency.

**Introduction:** The Sample Analysis at Mars (SAM) instrument on the Mars Science Laboratory (MSL) Curiosity rover will be able to measure sulfur isotope ratios of Martian samples *in-situ* [1]. Microbial sulfate reduction leaves a characteristic ‘biosignature’ behind in the isotopic composition of its metabolic reactants and products. The measurement capabilities of SAM should be able to address questions of past Martian habitability for sulfate-reducing microbes.

One issue with this approach is that the strongest isotopic signals are often preserved in sulfide minerals, which may not be long-lived in the oxidizing surface environment of Mars. However, previous research suggests that the S isotope composition of the parent sulfides should be indistinguishable from their oxidative products [2]. This sulfur isotope consistency implies that potential S isotope biosignatures may be preserved in Martian sulfates despite the intense oxidation on the surface of Mars.

In order to constrain the sulfur isotope characteristics of oxidative processes in cold dry environments, we studied the sulfur isotope systematics of mineralized sulfate-bearing crusts on sedimentary pyrite nodules from Devon Island, Canadian Arctic. These crusts display similarities to rocks studied by the Mars Exploration Rovers, including the coexistence of Ca-Mg-Fe sulfates with Fe-oxides and nanophase ferric oxides [3].

### *Geological Background*

Devon Island, Nunavut, is the fourth largest island in the Canadian Arctic Archipelago. It hosts a 23-km diameter impact crater—the Haughton Impact structure—that formed at  $39 \pm 2$  Ma [4]. The Paleozoic sedimentary package hosting the Haughton Impact structure contains thick sequences of carbonates and Ordovician sulfate evaporites, which gave rise to the carbonate- and sulfate-rich melt rocks within the crater [5]. After a period of exposure and erosion, lacustrine sediments were deposited in the crater during the Miocene Epoch [6] [7]. Presently 15 km<sup>2</sup> of the resulting Haughton Formation are exposed on the surface consisting of dolomitic silt, limestone, sandstone and ironstone [8] [9]. Within the dolomitic silt of the Haughton Formation there are pyrite nodules ranging from several cm up to 10s of cm across. The mineralogy of these nodules includes pyrite, gypsum, goethite, schwertmannite and jarosite [3].



**Figure 1:** Cross section of nodules from Devon Island. Image on left shows a more oxidized nodule. Image on right is primarily pyrite and with a gypsum coating. Penny for scale.

**Methods:** We collected nodules of varying degrees of oxidation from dolomitic silts of the Haughton Formation. Less oxidized nodules are grey to black in colour. The mineralogy of these nodules is primarily pyrite with a minor coating of gypsum. More oxidized nodules are less competent, reddish orange coloured, and dusted with a coating of yellow powder. Powder X-ray diffraction shows that they consist primarily of gypsum, goethite and jarosite-group minerals. Both potassium and hydronium jarosite are present but rarely occur in samples with pyrite present [3].

Twelve nodules, ranging from mostly pyrite to no pyrite, were powdered and bulk sulfide and sulfate were chemically extracted from each powder. The sulfur from the extraction procedures was trapped as Ag<sub>2</sub>S. Approximately 3 mg of Ag<sub>2</sub>S were then fluorinated to produce SF<sub>6</sub>. The resulting SF<sub>6</sub> was purified and analyzed for its multiple sulfur isotope composition on a ThermoFinnigan MAT 253 mass spectrometer.

**Results:** Sulfide  $\delta^{34}\text{S}$  values are uniformly negative, and range from -15‰ to -5‰ V-CDT. The associated  $\Delta^{33}\text{S}$  values are uniformly positive, and vary from 0.09‰ to 0.18‰ V-CDT. The characteristics are typical of pyrites produced from H<sub>2</sub>S from microbial sulfate reduction [10]. Sulfate  $\delta^{34}\text{S}$  values span a greater range ( $\approx 25\%$ ), from -10‰ to 15‰ V-CDT. The associated  $\Delta^{33}\text{S}$  values are uniformly positive, and vary from 0.05‰ to 0.19‰ V-CDT. In a majority of samples, sulfate has different  $\delta^{34}\text{S}$  or  $\Delta^{33}\text{S}$  values from the sulfide in the same nodule. This is unexpected since sulfide oxidation is typically accompanied by little to no isotopic fractionation.

**Discussion:** The unusual sulfide-sulfate isotope systematics may indicate a novel fractionation mechanism during low temperature oxidation. However, the

rocks underlying, and within, the Haughton Impact structure contain mobile sulfate. The sulfate we measured may reflect a mixture of sulfate produced during sulfide oxidation with this exogenous sulfate source. In order to evaluate this possibility, we constructed a two-component mixing model between sulfate derived from the sulfide in the nodules and sulfate derived from evaporite beds underlying the Haughton Impact structure. The sulfur isotopic composition of the bedrock gypsum, measured at  $\delta^{34}\text{S} = 28.7 \pm 3.6 \text{ ‰}$ , is typical of Ordovician seawater. [11]. We used a  $\Delta^{33}\text{S}$  value of  $-0.006 \pm 3.6 \text{ ‰}$  for the model calculations based on values for early Paleozoic seawater sulfate [12]. Since the sulfate within the Haughton melt rocks is sourced from these evaporites, our choice of this isotopic end member should be representative of this mixing end member as well.

The composition of the mixture is defined by the following equations:

$$\begin{aligned} {}^{34}R_{\text{mixture}} &= f_{\text{evaporite}}^S {}^{34}R_{\text{evaporite}} + f_{\text{sulfide}}^S {}^{34}R_{\text{sulfide}} \\ {}^{33}R_{\text{mixture}} &= f_{\text{evaporite}}^S {}^{33}R_{\text{evaporite}} + f_{\text{sulfide}}^S {}^{33}R_{\text{sulfide}} \\ 1 &= f_{\text{evaporite}}^S + f_{\text{sulfide}}^S \end{aligned}$$

In these equations,  ${}^{33}R_i$  and  ${}^{34}R_i$  represent  ${}^{33}\text{S}$ - ${}^{32}\text{S}$  and  ${}^{34}\text{S}$ - ${}^{32}\text{S}$  ratios, normalized to the V-CDT scale, and  $f_{\text{evaporite}}^S$  and  $f_{\text{sulfide}}^S$  represent the relative amount of sulfur in the mixture coming from the evaporite and sulfide end members. We constructed sample-specific mixing curves for each sulfide-sulfate pair by varying  $f_{\text{evaporite}}^S$  between 0 and 1.

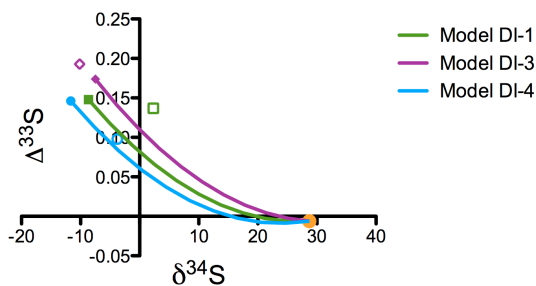


**Figure 2:** Solid symbols represent measured sulfide, while hollow symbols are measured sulfate. Lines are two-component mixing models between pyrite from nodules and bedrock gypsum. Orange circle is the gypsum bedrock.

Our samples fall into three types based on the relationship between the measured sulfate  $\delta^{34}\text{S}$  and  $\Delta^{33}\text{S}$  values (Figure 2). Type 1 has similar  $\delta^{34}\text{S}$  and  $\Delta^{33}\text{S}$  values between sulfide and sulfate (1 sample). In type 2 samples, measured sulfate  $\delta^{34}\text{S}$  and  $\Delta^{33}\text{S}$  values plot within error of the mixing curve (2 samples). Type 3 samples

have measured sulfate  $\delta^{34}\text{S}$  and  $\Delta^{33}\text{S}$  values that either fall below (2 samples) or above (7 samples) the mixing curve.

The sulfate  $\delta^{34}\text{S}$  and  $\Delta^{33}\text{S}$  values from the type 1 sample look like the conventional isotopic expectations for sulfide oxidation. A similar process, modified by mixing ~18-30% sulfate from local bedrock, can explain the isotopic composition of the two type 2 samples. Solute transport in cold-region groundwater can occur through a series of freeze, thaw and evaporation cycles [13], and would be especially effective if the transporting solutions were sulfate-rich brines. However, 30% sulfate is quite a substantial amount of sulfate to be transported from the bedrock evaporites. The most striking result of our modelling is that the majority of sulfate  $\delta^{34}\text{S}$  and  $\Delta^{33}\text{S}$  values cannot be explained by conventional sulfide oxidation.

We have found no simple relationship between sample type and visual indications of extent of oxidation (Figure 1). The type 3 oxidative process appears to operate in parallel with conventional sulfide oxidation rather than in some sort of redox sequence. Strong isotopic fractionations are characteristic of type 3 sulfide-sulfate pairs, where the sulfate is enriched in  ${}^{34}\text{S}$  by ~7-18‰ relative to the starting sulfide. This type of enrichment is also seen in sulfate-sulfide pairs at isotopic equilibrium. The exponential factor ( ${}^{33}\lambda$ ) that relates  ${}^{33}\text{S}$ - ${}^{32}\text{S}$  fractionations to  ${}^{34}\text{S}$ - ${}^{32}\text{S}$  fractionations is lower than that expected from isotopic equilibrium in the majority of type 3 samples, with an average  ${}^{33}\lambda$  value of  $0.5129 \pm 0.0018$  (1SD) for the 7 samples that plot above their respective mixing curves. While we do not yet have a full understanding of the oxidative mechanism behind these unique fractionations, their existence has clear implications for investigating potential biosignatures on the surface of Mars. If an isotopic enrichment of 10-20‰ can be produced by low-temperature sulfide oxidation, preservation of potential records of microbial sulfate reduction may be incompatible with the present Martian surface environment, or for that matter, much of its climatic history.

#### References:

- [1] Franz, H.B., et al. (2011) *LPS XL11*, 2800-2801.
- [2] Seal II, R.R. (2006) *Reviews in Min. and Geochem.*, 633-677.
- [3] L veill , R. (2007) *GSA*
- [4] Sherlock, S.C., et al. (2005) *Meteoritics & Planet. Sci.*, 40, 1777-1787.
- [5] Osinski, G. & Spray, J. (2003) *Earth and Planet. Sci. Letters*, 215, 357-370.
- [6] Osinski, G.R., et al. (2005) *Meteoritics & Planet. Sci.*, 40, 1759-1776.
- [7] Hickey, L.J., et al. (1988) *Meteoritics*, 23, 221-231.
- [8] Osinski, G.R. and Lee, P. (2005) *Meteoritics & Planet. Sci.*, 40, 1887-1899.
- [9] Mayr, R.T. (1987) *The Sedimentary Rocks of Devon Island*. [10] Ono, S., et al. (2006). *GCA.*, 70, 2238-2252.
- [11] Parnell, J., et al. (2010) *Geology*, 38, 271-274.
- [12] Wu, N., et al. (2010) *GCA.* 74, 2053-2071.
- [13] Lacelle, D. & L veill , R. (2010) *Planet. and space sci.*, 2010. 58, 509-522.